Active power control of waked wind farms

van Wingerden, Jan Willem; Pao, Lucy; Aho, Jacob; Fleming, Paul

DOI
10.1016/j.ifacol.2017.08.378

Publication date
2017

Document Version
Final published version

Published in
IFAC-PapersOnLine

Available online at www.sciencedirect.com

ScienceDirect

IFAC PapersOnLine 50-1 (2017) 4484–4491

Active Power Control of Waked Wind Farms ⋆

Jan-Willem van Wingerden * **Lucy Pao** ** **Jacob Aho** ** **Paul Fleming** ***

* *Delft University of Technology, Delft, 2628CD The Netherlands tel:+31 15 2781720, e-mail: j.w.vanwingerden@tudelft.nl*
** *University of Colorado, Boulder, CO 80309 USA tel: +1 303 492 2360, e-mail: pao@colorado.edu*
*** *National Renewable Energy Laboratory, Golden, CO 80401 USA tel: +1 303 384 6918, e-mail: paul.fleming@nrel.gov*

Abstract: Active power control can be used to balance the total power generated by wind farms with the power consumed on the electricity grid. With the increasing penetration levels of wind energy, there is an increasing need for this ancillary service. In this paper, we show that the tracking of a certain power reference signal provided by the transmission system operator can be significantly improved by using feedback control at the wind farm level. We propose a simple feedback control law that significantly improves the tracking behavior of the total power output of the farm, resulting in higher performance scores. The effectiveness of the proposed feedback controller is demonstrated using high-fidelity computational fluid dynamics simulations of a small wind farm.

Keywords: Wind farm control, control of renewable energy resources, analysis and control in deregulated power systems, control system design, wind energy

1. INTRODUCTION

Wind energy is expected to be the largest European source of energy by 2030 and is therefore largely responsible for enabling Europe to achieve its goal of having at least 27% of its electrical energy generated by renewable sources [Pineda, 2015]. However, the present high costs of offshore wind energy inhibit further deployment of large-scale offshore wind power plants. The uncertainty of the power output of a wind farm also adds to utility grid power balancing costs. This uncertainty is caused by, among other factors, the variability of the wind flow within a wind farm [van Kuik et al., 2016]. Nonetheless, with an increased understanding of flow dynamics, better forecasts can be made of the available wind power in a farm and in combination with control strategies, wind farms should even be able to provide grid balancing services [Boersma et al., 2017]. With ever-increasing penetration levels of wind energy, there will be a need for this ancillary service.

Using active control to balance the total power generated with the power consumed on the grid is called active power control (APC). There are several types of APC [Aho et al., 2013]. In this paper, we focus on automatic generation control (AGC), or frequency regulation, in which the wind farm should track a power reference signal provided by the transmission system operator (TSO). This typically means that a certain power reserve should be present with respect to the available power within a wind farm. An implementation of a single-turbine controller capable of providing power reserve and AGC response is given in Aho et al. [2013, 2016].

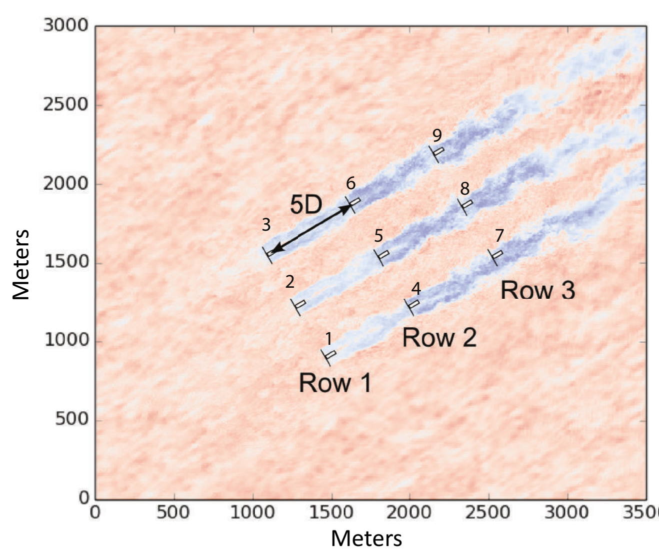

Fig. 1. Layout of the simulated 3-by-3 wind farm. Background is an instantaneous horizontal slice of flow output taken from a Simulator fOr Wind Farm Applications (SOWFA) simulation for the "high-waking" situation. Turbine rows and individual turbine numbers are indicated.

Fleming et al. [2016] present an initial computational fluid dynamics (CFD) simulation study of AGC being provided at a wind farm level. In that paper, the turbines are coordinated through an open-loop supervisory controller that evenly derates the turbines and evenly distributes the power set point requirements to the individual turbines. The goal of the control problem is to track an AGC signal that can specify an increase

⋆ J.W. van Wingerden would like to acknowledge the CL-Windcon project. This project has received funding from the European Union Horizon 2020 research and innovation programme under grant agreement No 727477. L. Pao gratefully acknowledges funding provided by the Hanse-Wissenschaftskolleg Institute for Advanced Study, Delmenhorst, Germany. J. Aho has been supported in part by the Renewable and Sustainable Energy Institute and a University of Colorado Boulder Graduate School Summer Fellowship.

2405-8963 © 2017, IFAC (International Federation of Automatic Control) Hosting by Elsevier Ltd. All rights reserved.
Peer review under responsibility of International Federation of Automatic Control.
10.1016/j.ifacol.2017.08.378

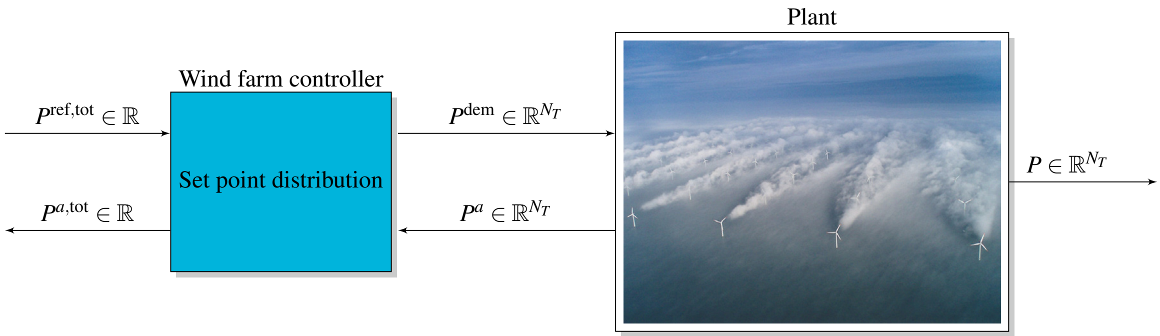

Fig. 2. General overview of the wind farm controller (includes photograph of the Horns Rev 1 offshore wind farm, Christian Steiness).

and/or decrease relative to the nominal de-rated power. Each individual turbine has its own local feedback controller to track its own power reference set point. To track an increasing power reference, it is necessary to have enough power in reserve. If all turbines are de-rated equally, this requires de-rating to a level such that all the turbines have enough wind power in reserve.

Two cases were evaluated in Fleming et al. [2016] for a 3-by-3 wind farm (as shown in Fig. 1 for the "high-waking" case). In the first "low-waking" case, the wind direction was chosen such that the amount of turbine-to-turbine waking was very limited. In the second "high-waking" case, the wake interaction was strong. In that paper, each turbine is de-rated to the same level and is tasked with individually providing one-ninth of the required AGC response.

In the "low-waking" case, this approach yielded very good wind farm power tracking performance. As discussed in Aho et al. [2016], individual turbines are capable of good AGC responses if enough wind is available, and further, the "low-waking" results demonstrate that the aggregate wind farm power is better than any individual turbine in terms of grid performance scores. However, we do note that the performance could be further improved. The turbulent flow includes lulls occurring spatially that cause durations of low power on some turbines, which could be compensated for if other turbines responded to this situation.

In the "high-waking" case, this open-loop approach of even de-rating and power set point distribution was found to be unacceptable. It is difficult to choose an appropriate uniform open-loop reserve level for the entire farm, such that each turbine can meet its power reference because of the turbine-to-turbine interaction through wakes. Feedback control at the wind farm level could significantly improve the wind farm power tracking performance by effectively changing the individual turbine power set points to address wind lulls that may occur in one part of the farm.

Recent papers that have proposed feedback to optimize the local set points have assumed that the individual turbines have enough available power to track their set point [Madjidian, 2016, Hansen et al., 2006, Spudic et al., 2010]. In this paper, we consider the "high-waking" case, wherein on average there is enough available power to track the set point. However, as a result of local effects, some individual turbines fail to follow their set points. It is evident from Fleming et al. [2016] that two problems need to be solved to deliver a quality AGC response in the "high-waking" case. The first is set point selection and the distribution thereof, and the second is the design of a wind farm feedback controller that can appropriately adjust the turbine set points to address underperformance (due to lulls) that may be occurring at some turbines. The main contribution of this paper is a simple feedback controller that leads to good wind farm power tracking performance in "high-waking" scenarios for different distributions of the AGC set point.

The outline of this paper is as follows. Set point selection is discussed in Section 2, and a simple wind farm feedback controller is presented in Section 3. In Section 4, CFD simulation results in a "high-waking" scenario show that feedback can significantly improve the wind farm power tracking performance. The paper is concluded in Section 5.

2. SET POINT SELECTION

As stated in the introduction, in order to have the total power output of the wind farm follow a demanded trajectory, an overall wind farm controller must coordinate the power set points of the individual turbines such that their power production sums to the desired amount. The coordination is made complicated when the turbines interact through wake losses.

Given the wind direction and speed, a set point selection algorithm must

(1) estimate the total power available now and in the immediate future,
(2) from this, determine the plant-wide power reserve level needed to provide AGC reliably well, and
(3) determine the optimal collection of set points to distribute to the individual turbines.

These steps most likely must be done through reference to a continuously updated wake model. This process is the subject of the EU PossPow project [Bozkurt et al., 2014].

Choosing the optimal collection of set points is a challenge, as the interaction between wake models and changes in power set points / axial induction is still active research (see Annoni et al. [2016], and Vali et al. [2016]). In Fig. 2, a simple (ideal) wind farm control architecture is presented that is used by many others (e.g., Madjidian [2016], Hansen et al. [2006], Spudic et al. [2010]). The wind farm controller receives the power generation command in combination with the AGC command from the TSO, also denoted as the overall power reference, $P^{\text{ref,tot}} \in \mathbb{R}$, while the wind farm controller communicates back a predicted available power, $P^{a,\text{tot}} \in \mathbb{R}$, of the whole wind farm by using, for example, a dynamic model in combination with a Kalman filter [Boersma et al., 2016, Doekemeijer et al., 2016].

Note that predicted available power can be higher than the power produced by the farm because it might already be de-rated.

The task of the wind farm controller is to distribute the AGC set point over N_T turbines, $P^{\text{dem}} \in \mathbb{R}^{N_T}$, where each turbine has its own local feedback controller to track individual power demand. Based on possible wake interaction or availability of the different turbines, the true optimal solution is generally a heterogeneous one. The wind farm controller has to distribute this set point based on an estimate of the available power at every turbine, denoted by $P^a \in \mathbb{R}^{N_T}$. The estimation of the available power at a timescale of seconds is a rather challenging task [Bozkurt et al., 2014]. However, on longer timescales, these estimates become better. We can conclude that the estimation of the available power is a challenging problem because of the largely unpredictable nature of wind at a faster timescale. Uncertainty is typically the reason to employ a feedback controller, which is the topic of the next section.

If a wind farm is de-rated, there are several ways to de-rate the individual turbines. In this paper, we will show two de-rating cases and how the closed-loop performance with respect to power reference tracking is similar. However, the loading of the individual turbines can be significantly different. This aspect further complicates the distribution of the set point problem.

3. FEEDBACK CONTROL

As described in the previous section, the uncertainty of the predictions on a faster timescale can be resolved by using feedback. Feedback control can be used to combat local turbulence-driven wind lulls that deviate from the mean wind speeds estimated by the wake models. Here, we propose a simple feedback controller that improves the tracking performance of the wind farm.

The main idea is to let the N_T turbines in the wind farm work together. The proposed control architecture is shown in Fig. 3, where $\Delta P^{\text{ref}} \in \mathbb{R}^{N_T}$ is the control signal that may increase the set points of the individual turbines. The overall power $P^{\text{tot}} \in \mathbb{R}$ is defined as $P^{\text{tot}} = \mathbf{1}_{1\times N_T} P = \sum_{i=1}^{N_T} P_i$, and the overall power reference $P^{\text{ref,tot}} \in \mathbb{R}$ is defined $P^{\text{ref,tot}} = \sum_{i=1}^{N_T} P_i^{\text{ref}}$, where $\mathbf{1}_{1\times N_T}$ is defined as $[1\ 1\ \cdots\ 1] \in \mathbb{R}^{1\times N_T}$ and $\mathbf{1}_{N_T\times 1} = \mathbf{1}^T_{1\times N_T}$. The vector $e \in \mathbb{R}^{N_T}$ contains the set point errors of the individual turbines, whereas $e^{\text{tot}} = P^{\text{ref,tot}} - P^{\text{tot}} \in \mathbb{R}$ is the overall tracking error of the wind farm. As explained in the previous section, it is not always possible to follow the local set points because of wake effects or the turbulent nature of the wind. However, the TSO is only interested in the wind farm power following the overall reference $P^{\text{ref,tot}}$. The proposed controller is only active if there is an overall tracking error. If there is a overall tracking error caused by one or more turbines not following their individual power references, the controller will distribute this overall error among all the turbines.

In the remainder of this section, we present a simple model structure for analysis and controller design. This information is followed by an explanation of the proposed feedback controller and the need for gain scheduling.

3.1 Simple Model for Controller Synthesis

Before we explain the proposed controller in more detail, we will describe a simple model of the wind farm. We assume that every turbine in the wind farm is able to track its reference signal with a certain bandwidth. This ability results in the following simple model for turbine i

$$\frac{P_i}{P_i^{\text{dem}}} = G_i(s) = \frac{K_i\omega^2}{s^2 + 2\beta\omega s + \omega^2} \tag{1}$$

where ω is the bandwidth of the local feedback controller and K_i is the gain of the i^{th} turbine. The gain, $K_i \le 1$, of the i^{th} turbine is assumed to be 1 if there is locally enough power available to track the reference signal. If there is not enough wind power available, the local gain will drop, $K_i < 1$. We also define the following multi-input multi-output transfer function

$$\underbrace{\begin{bmatrix} P_1 \\ P_2 \\ \vdots \\ P_{N_T} \end{bmatrix}}_{P\in\mathbb{R}^{N_T}} = \underbrace{\begin{bmatrix} G_1 & 0 & \dots & 0 \\ 0 & G_2 & & 0 \\ \vdots & & \ddots & \\ 0 & 0 & & G_{N_T} \end{bmatrix}}_{G^{farm}\in\mathbb{R}^{N_T\times N_T}} \underbrace{\begin{bmatrix} P_1^{\text{dem}} \\ P_2^{\text{dem}} \\ \vdots \\ P_{N_T}^{\text{dem}} \end{bmatrix}}_{P^{\text{dem}}\in\mathbb{R}^{N_T}} \tag{2}$$

In this model structure, we ignore possible dynamic interactions between the individual turbines. This assumption is allowed, because the time-varying dynamic wake interaction is present at a slower timescale and consequently does not affect the closed-loop performance of the proposed wind farm feedback controller.

The total tracking error is defined as

$$e^{\text{tot}} = \sum_{i=1}^{N_T}\left(P_i^{ref} - P_i\right) = \mathbf{1}_{1\times N_T}\left(P^{\text{ref}} - P\right) \tag{3}$$

In the case of no feedback control, $K(s) = 0$ and $P^{\text{dem}} = P^{\text{ref}}$, and using (1) and (3), the overall tracking error is given by

$$e^{\text{tot}}_{\text{OL}} = \sum_{i=1}^{N_T} \frac{\left(s^2 + 2\beta\omega s + (1-K_i)\omega^2\right)}{s^2 + 2\beta\omega s + \omega^2} P_i^{\text{ref}}. \tag{4}$$

The steady-state gain from P_i^{ref} to $e^{\text{tot}}_{\text{OL}}$ is determined by taking the limit as $s \to 0$ and is

$$\sum_{i=1}^{N_T}(1-K_i) \tag{5}$$

In the case in which all the turbines have enough available power, $K_i = 1\ \forall i$, and the total tracking error is zero in steady state.

In the remainder of this section, we propose, a simple gain-scheduled proportional-integral (PI) controller and compare the tracking performance with the situation without feedback.

3.2 Proportional-Integral Controller

For the PI controller, we use the control architecture as given in Fig. 3. This configuration has a single-input single-output feedback controller, $K(s)$. With this definition and the configuration given, we can derive the overall tracking error as a function of the individual power reference set points:

$$\begin{aligned} e^{\text{tot}}_{CL} &= \mathbf{1}_{1\times N_T}\left(P^{\text{ref}} - G^{\text{farm}}(s)\left(P^{\text{ref}} + \mathbf{1}_{N_T\times 1}K(s)e^{\text{tot}}_{CL}\right)\right) \\ &= \mathbf{1}_{1\times N_T}\left(P^{\text{ref}} - G^{\text{farm}}(s)P^{\text{ref}} - G^{\text{farm}}(s)\mathbf{1}_{N_T\times 1}K(s)e^{\text{tot}}_{CL}\right) \\ &= \frac{\sum_{i=1}^{N_T}\frac{\left(s^2+2\beta\omega s+(1-K_i)\omega^2\right)}{s^2+2\beta\omega s+\omega^2}P_i^{\text{ref}}}{1+\sum_{i=1}^{N_T}\frac{K_i\omega^2}{s^2+2\beta\omega s+\omega^2}K(s)} \end{aligned} \tag{6}$$

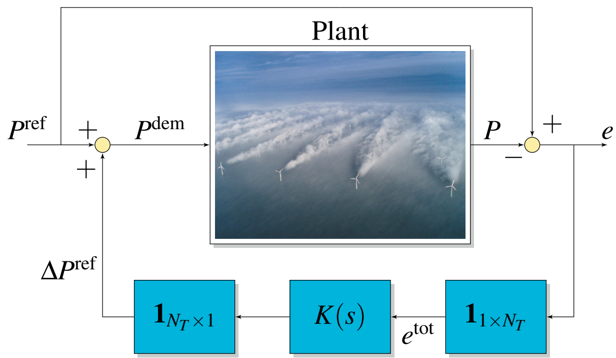

Fig. 3. Schematic representation of the wind farm feedback control system (includes photograph of the Horns Rev 1 offshore wind farm, Christian Steiness).

The steady-state gain from P_i^{ref} to $e_{\mathrm{CL}}^{\mathrm{tot}}$ is similarly determined by taking the limit as $s \to 0$ and is

$$\lim_{s\to 0} \frac{\sum_{i=1}^{N_T}(1-K_i)}{1+\sum_{i=1}^{N_T} K_i K(s)} \tag{7}$$

If there is locally enough power available for every turbine, the numerator of this expression will become zero.

The performance of the feedback controller can be evaluated by comparing the total tracking error when there is feedback to when there is no feedback. For this purpose, we define the following sensitivity function

$$S(s) = \frac{e_{CL}^{\mathrm{tot}}}{e_{OL}^{\mathrm{tot}}} = \frac{1}{1+\sum_{i=1}^{N_T} \frac{K_i\omega^2}{s^2+2\beta\omega s+\omega^2} K(s)} \tag{8}$$

Like a normal sensitivity function, this equation has the following interpretation.

(1) If $S(s) < 1$, the feedback controller will reduce the tracking error compared to the open-loop situation.
(2) If $S(s) = 1$, there is no effect caused by the feedback controller.
(3) If $S(s) > 1$, the feedback controller will increase the tracking error compared to the open-loop situation.

Because of the Bode sensitivity integral and stability considerations, it is not possible to have only $S(s) < 1$. In the remainder of this section, we discuss the stability of the proposed control architecture, steady-state performance, bandwidth, and the need for gain scheduling.

We propose the following PI controller

$$K(s) = K_p + \frac{K_I}{s} \tag{9}$$

where the controller gains might be gain-scheduled. For the remainder of this subsection, we assume that the controller gains are constant. With the given PI controller, the sensitivity is given by

$$S(s) = \frac{s^3+2\beta\omega s^2+\omega^2 s}{s^3+2\beta\omega s^2+\omega^2 s+\omega^2\sum_{i=1}^{N_T} K_i\,(K_p s+K_I)} \tag{10}$$

The steady-state gain of this sensitivity function equals zero, $S(0) = 0$, which implies that in steady state the closed-loop tracking error is zero. For the problem at hand, this can only be true if the available power in the farm is sufficient to track the overall reference signal.

The following is the characteristic polynomial of (10)

$$s^3+2\beta\omega s^2+\omega^2\left(1+K_p'\right)s+K_I'\omega^2 \tag{11}$$

with $K_p' = \sum_{i=1}^{N_T} K_p K_i$ and $K_I' = \sum_{i=1}^{N_T} K_I K_i$. Using the Routh-Hurwitz stability criterion, for closed-loop stability, we must have

$$K_I' < 2\beta\omega\left(1+K_p'\right) \tag{12}$$

Assuming all the turbines have enough power available (so $K_i = 1\ \forall i$) and setting $K_p = \frac{1}{N_T}$ (which is saying that we cannot exceed the bandwidth of the local active power controller), we obtain

$$K_I < \frac{4\beta\omega}{N_T} \tag{13}$$

In the case in which one of the turbines does not have enough power, the overall gain of the system will drop, resulting in a lower loop gain that still yields stability but also a lower bandwidth. Therefore, we propose a gain-scheduled feedback controller in the next subsection.

3.3 Gain-Scheduled Proportional-Integral Controller

The main objective of the feedback controller is to bring the total tracking error back to zero. The PI controller achieves this because of the high gain that results at low frequencies. In this section, we propose a gain-scheduled proportional-integral controller that keeps the bandwidth of the controller constant.

The loop gain will significantly drop when some turbines cannot achieve their set points because of insufficient winds at their locations. To drive e^{tot} to zero, we increase the set points of all of the turbines, but only the turbines that still have power available will actually be able to contribute. Linearizing the dynamics of the individual turbines, and considering the changes to the steady-state behavior, this mathematically translates into

- $\frac{\partial P_i}{\partial P_i^{\mathrm{dem}}} = 1$, if turbine i has enough power available
- $\frac{\partial P_i}{\partial P_i^{\mathrm{dem}}} = 0$, if turbine i does not have enough power available

This linearization affects both the stability conditions as well as the bandwidth of the system. By keeping the loop gain constant, which is a function of the "active" turbines, will guarantee stability and the same bandwidth of the system. With a simple thresholding procedure, the number N_S of turbines is estimated that cannot follow their local set point. Then, the gain-scheduled PI controller is

$$K(s) = K_p^{gs} + \frac{K_I^{gs}}{s} \tag{14}$$

where the gains are

$$K_p^{gs} = \min\left(\frac{N_T}{N_T-N_S}, N_T\right) K_p \tag{15}$$

$$K_I^{gs} = \min\left(\frac{N_T}{N_T-N_S}, N_T\right) K_I \tag{16}$$

where K_p and K_I are the originally designed proportional and integral gains from Section 3.2. Depending on N_S, these gains are increased as needed to maintain the loop gain of the system. The performance of this gain-scheduled feedback controller is evaluated in the next section.

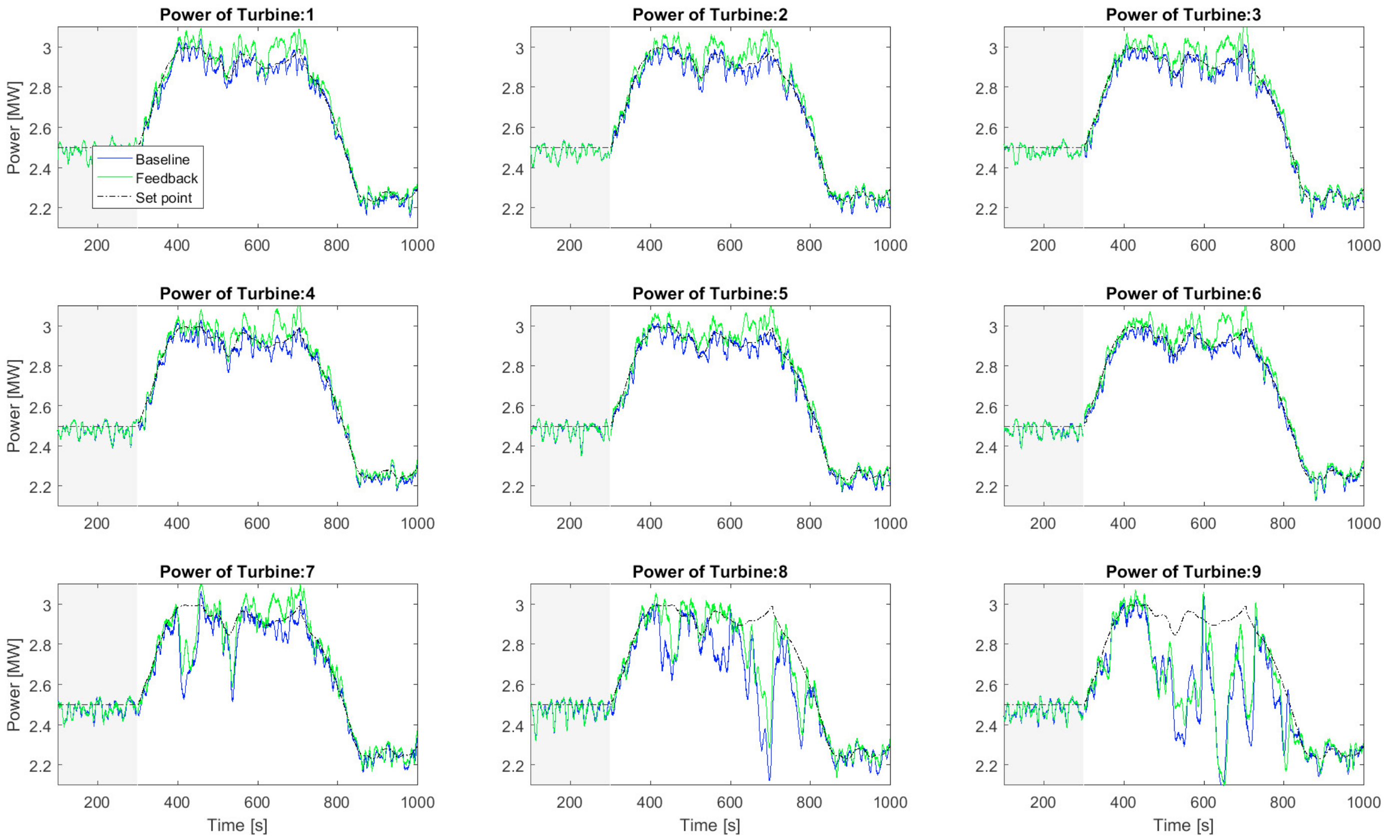

Fig. 4. Power of the individual wind turbines within the farm with and without the proposed feedback control where we track the reference signal for the 50-50-50 case. In the feedback cases, the feedback is activated only after 300 seconds.

4. SIMULATOR FOR WIND FARM APPLICATIONS SIMULATIONS

To evaluate the final gain-scheduled, closed-loop wind farm controller of Section 3.3, we use the Simulator fOr Wind Farm Applications (SOWFA) tool [Churchfield and Lee, 2015] developed by the National Renewable Energy Laboratory (NREL). SOWFA uses an actuator line model coupled with NREL's FAST wind turbine simulator [Jonkman and Buhl Jr., 2005] to compute the dynamic response of wind turbines in the atmospheric boundary layer. Specifically, SOWFA uses large eddy simulation methods to solve the three-dimensional incompressible Navier-Stokes equations and transport of potential temperature equations, which take into account the thermal buoyancy and Earth rotation (Coriolis) effects in the atmosphere. SOWFA calculates the unsteady flow field to compute the time-varying power, velocity deficits, and loads at each turbine in a wind farm.

The wind farm simulated is shown in Fig. 1 using an image taken from one time step of a horizontal slice of the CFD flow. The wind farm is composed of nine NREL 5-MW reference turbines [Jonkman et al., 2009] arranged in a regular 3-by-3 grid with a spacing of 630 m, which is equal to 5 rotor diameters (5D). The domain size is 3 km by 3.5 km by 1 km to allow for sufficient distance surrounding the turbines so that boundary effects are negligible at the turbines.

In Fleming et al. [2016], different set points are considered for the "high-waking" case. In this paper, we used similar scenarios that are defined by the set points of the three rows as defined in Fig. 1. We distribute the overall power reference over the different rows, where the local reference signals are expressed in the available power in the unwaked situation. We consider an average wind speed of 12 m/s and the following scenarios:

- Case 50-50-50: Every turbine is de-rated to 50% of the rated power
- Case 80-50-20: The first row is de-rated to 80% of the rated power, the second row to 50%, and the last row to 20%

Please note that the overall reference signal for the two situations is the same.

The results for the 50-50-50 case are given in Figs. 4-6 and for the 80-50-20 case in Figs. 7-9. In the 50-50-50 case, several lulls in the response of the turbines in row three can be

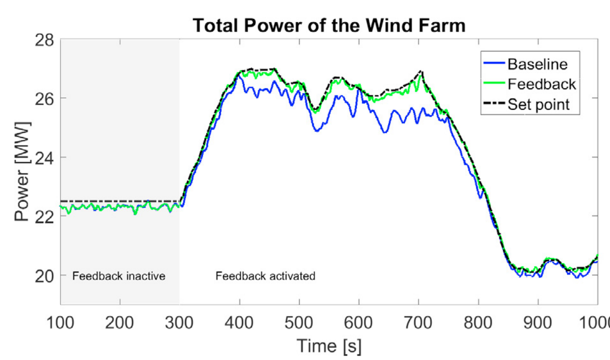

Fig. 5. Total power of the wind farm with and without the proposed feedback control, wherein we track the reference signal for the 50-50-50 case.

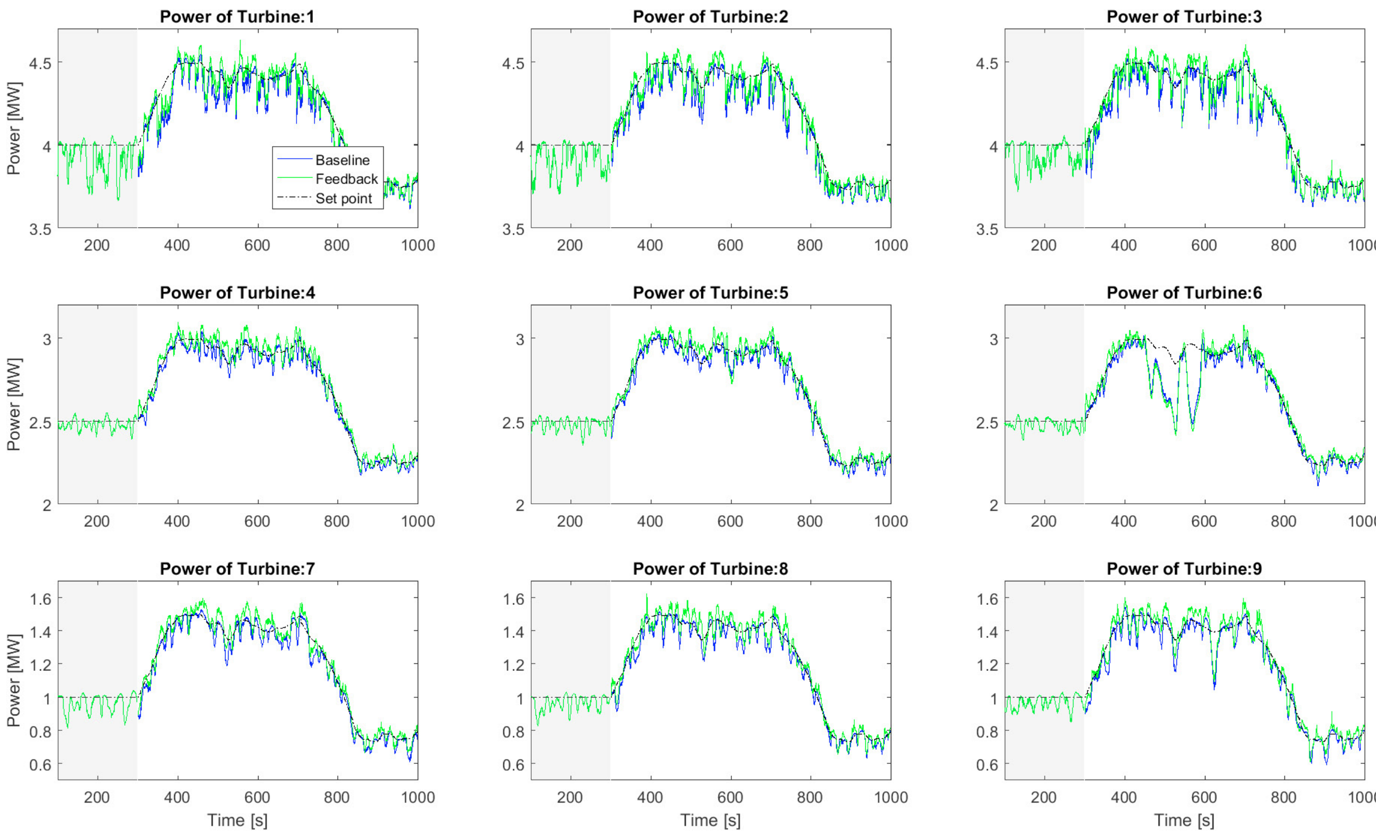

Fig. 7. Power of the individual wind turbines within the farm with and without the proposed feedback control, wherein we track the reference signal for the 80-50-20 case. In the feedback cases, the feedback is activated only after 300 seconds.

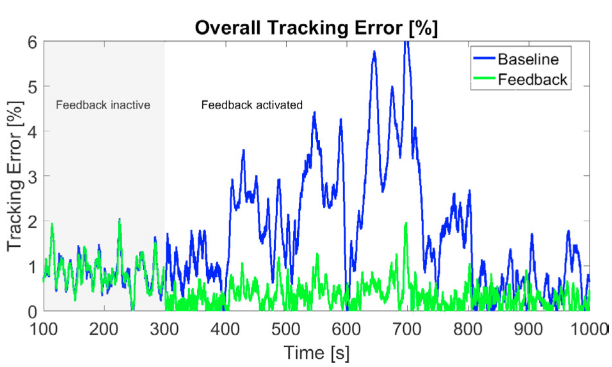

Fig. 6. Tracking error of the wind farm with and without the proposed feedback control, wherein we track the reference signal for the 50-50-50 case.

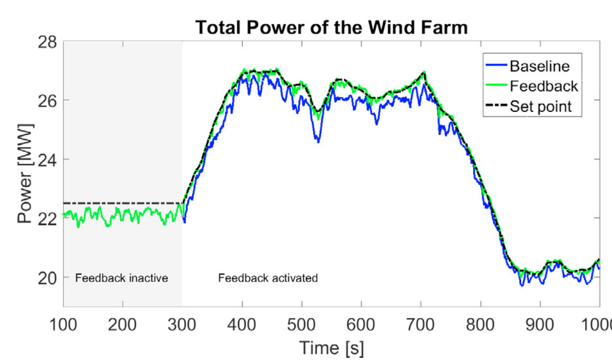

Fig. 8. Total power of the wind farm with and without the proposed feedback control, wherein we track the reference signal for the 80-50-20 case.

observed. The feedback controller increases the power capture of the other six turbines and the overall power set point can be tracked. For the 80-50-20 case, turbine 6 has a significant drop in available power, and the other turbines are able to compensate for this.

To assess the performance of the controller, two criteria are used:

- The first is the RMS of the tracking error, which tests the tracking capabilities of the feedback controller
- The second is the California Independent System Operator (CAISO) performance score, which rates power tracking between 0 and 1, as described in Aho et al. [2016]. Performance scores such as this are used in the US power markets to partially determine the payments for providing AGC services [CAISO, 2012]. This tests both that the set points were chosen to allow tracking, and additionally, the ability of feedback to improve aggregate tracking is tested here as well.

The results are presented in Table 1, where "Baseline" indicates the situation without feedback, and "Control" represents the situation with the gain-scheduled feedback controller. It is clear that feedback significantly reduces the RMS errors and improves CAISO scores for the two set point distributions, which would result in increased payments for the AGC services and improved grid reliability. A CAISO score above 0.5 is required to remain qualified to provide AGC ancillary services. Hence, we have shown that with feedback control, a "high-waking" wind farm can be used for AGC. Moreover, the total

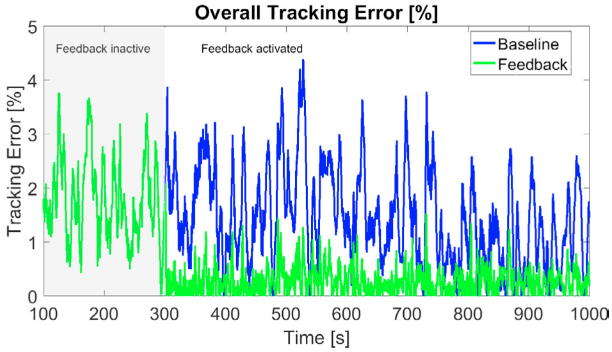

Fig. 9. Tracking error of the wind farm with and without the proposed feedback control, wherein we track the reference signal for the 80-50-20 case.

Table 1. Performance results

	RMS Error [W]	CAISO Accuracy Score [-]
Baseline 50-50-50	573670	0.81
Control 50-50-50	107000	0.93
Difference [%]	-81	14.8
Baseline 80-50-20	419330	0.84
Control 80-50-20	91554	0.94
Difference [%]	-78	11.9

power set points for the two cases are the same by construction. With feedback control, they have similar CAISO performance scores, though the 80-50-20 scenario leads to a somewhat lower RMS error.

Because the loading of the individual turbines is also important to wind farm operators, the damage equivalent load (DEL) [Hayman and Buhl Jr, 2012] of the out-of-plane bending moment is presented for the different turbines in the farm for the different scenarios in Fig. 10, where "control" denotes the situations in which feedback control is used. In Fig. 11, the DEL for the tower fore-aft bending moment is given. In general, the loading of the individual turbines increases slightly by using the proposed gain-scheduled feedback controller.

There are significant differences in the loading patterns for the two different cases. In the case of only considering the tower fore-aft bending moment, the 50-50-50 scenario is a better solution when considering structural loading because the loading is better distributed over the wind farm. When considering the out-of-plane bending moment, the 80-50-20 scenario is preferred.

5. CONCLUSIONS

We have shown that it is possible to successfully apply active power control for a "high-waking" wind farm to balance the total power generated with the power consumed on the grid. To establish this result, a simple gain-scheduled controller was presented and evaluated using high-fidelity computational fluid dynamics simulations. We also saw that changing the selection of the set points can yield different structural loading results, and this should be carefully considered in the overall wind farm active power controller design.

In the future we are going to look at the combined set point distribution and feedback problem for a variety of atmospheric conditions and larger layouts. Moreover, we are going to optimize the distribution of set points to minimize the overall loading on the farm for varying conditions.

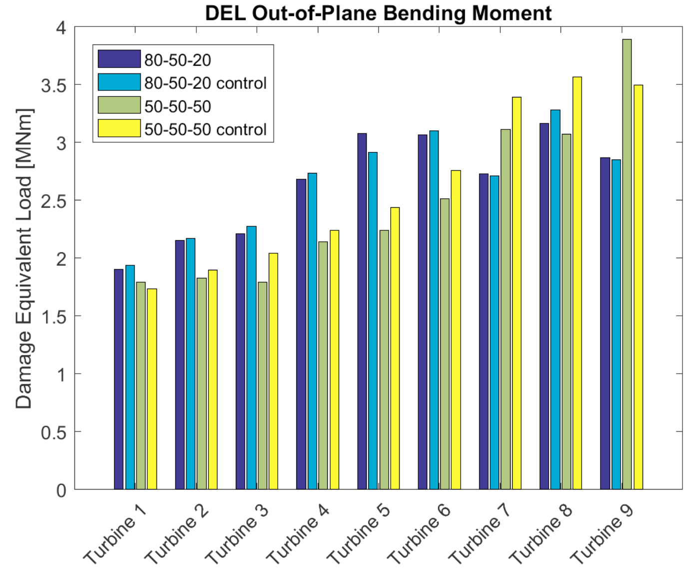

Fig. 10. Damage equivalent load of the out-of-plane bending moment for the different turbines and scenarios.

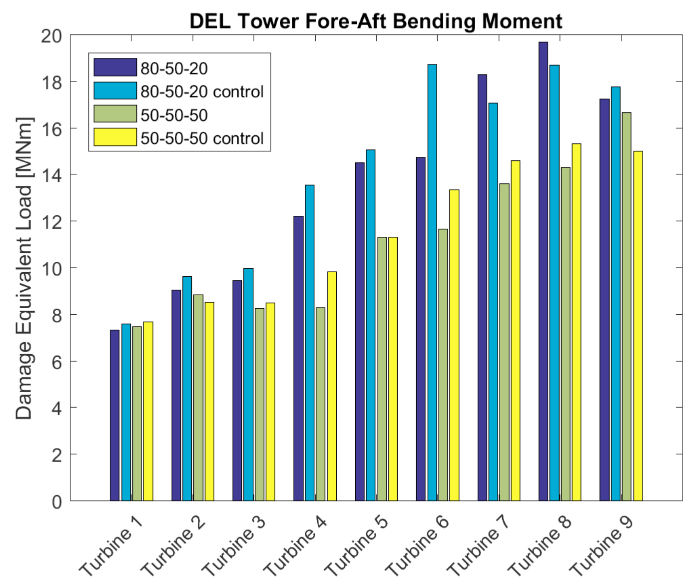

Fig. 11. Damage equivalent load of the fore-aft tower bending moment for the different turbines and scenarios.

REFERENCES

J. Aho, A. Buckspan, L. Y. Pao, and P. A. Fleming. An active power control system for wind turbines capable of primary and secondary frequency control for supporting grid reliability. In *51st AIAA Aerospace Sciences Meeting including the New Horizons Forum and Aerospace Exposition*, pages 1–13, 2013.

J. Aho, P. A. Fleming, and L. Y. Pao. Active power control of wind turbines for ancillary services: a comparison of pitch and torque control methodologies. In *American Control Conference*, pages 1407–1412, Boston, MA, 2016. ISBN 9781467386814.

J. Annoni, P. M. O. Gebraad, A. K. Scholbrock, P. A. Fleming, and J. W. van Wingerden. Analysis of axial-induction-based wind plant control using an engineering and a high-order wind plant model. *Wind Energy*, 2016.

S. Boersma, P. M. O. Gebraad, M. Vali, B. M. Doekemeijer, and J. W. van Wingerden. A control-oriented dynamic wind farm flow model: WFSim. In *Journal of Physics: Conference Series*, volume 753, page 032005. IOP Publishing, 2016.

S. Boersma, B. M. Doekemeijer, P. M. O. Gebraad, P. A. Fleming, J. Annoni, A. K. Scholbrock, J. A. Frederik, and J. W. van Wingerden. A tutorial on control-oriented modelling and control of wind farms. In *proceedings of the American Control Conference*, 2017.

T. G. Bozkurt, G. Giebel, N. K. Poulsen, and M. Mirzaei. Wind speed estimation and parametrization of wake models for down regulated offshore wind farms within the scope of PossPOW project. In *The Science of Making Torque from Wind*, volume 012156, 2014.

CAISO. Pay for performance regulation draft final proposal. Technical report, California Independent System Operator Corp., Folsom, CA, 2012.

M. Churchfield and S. Lee. NWTC information portal - SOWFA. 2015.

B. M. Doekemeijer, J. W. van Wingerden, S. Boersma, and L. Y. Pao. Enhanced Kalman filtering for a 2D CFD NS wind farm flow model. In *Journal of Physics: Conference Series*, volume 753, page 052015. IOP Publishing, 2016.

P. Fleming, J. Aho, P. M. O. Gebraad, L. Y. Pao, and Y. Zhang. CFD simulation study of active power control in wind plants. In *American Control Conference*, 2016.

A. D. Hansen, P. Sørensen, F. Iov, and F. Blaabjerg. Centralised power control of wind farm with doubly fed induction generators. *Renewable Energy*, 31(7):935 – 951, 2006.

G. J. Hayman and M. Buhl Jr. MLife user's guide for version 1.00. 2012.

J. Jonkman and M. L. Buhl Jr. FAST manual user's guide, NREL report no. NREL/EL-500-38230. August 2005.

J. Jonkman, S. Butterfield, W. Musial, and G. Scott. Definition of a 5-MW reference wind turbine for offshore system development. Technical report, NREL/TP-500-38060. Golden, CO: National Renewable Energy Laboratory, 2009.

D. Madjidian. Scalable minimum fatigue control of dispatchable wind farms. *Wind Energy*, 2016. doi: 10.1002/we.

I. Pineda. Aiming high: rewarding ambition in wind energy. *A position paper by the European Wind Energy Association*, 2015.

V. Spudic, M. Jelavic, M. Baotic, and N. Peric. Hierarchical wind farm control for power/load optimization. *The Science of Making Torque from Wind*, 2010.

M. Vali, J. W. van Wingerden, S. Boersma, V. Petrović, and M. Kühn. A predictive control framework for optimal energy extraction of wind farms. In *Journal of Physics: Conference Series*, volume 753, page 052013. IOP Publishing, 2016.

G. A. M. van Kuik, J. Peinke, R. Nijssen, D. Lekou, J. Mann, J. N. Sørensen, C. Ferreira, J. W. van Wingerden, D. Schlipf, P. Gebraad, H. Polinder, A. Abrahamsen, G. J. W. van Bussel, J. D. Sørensen, P. Tavner, C. L. Bottasso, M. Muskulus, D. Matha, H. J. Lindeboom, S. Degraer, O. Kramer, S. Lehnhoff, M. Sonnenschein, P. E. Sørensen, R. W. Künneke, P. E. Morthorst, and K. Skytte. Long-term research challenges in wind energy – a research agenda by the european academy of wind energy. *Wind Energy Science*, 1(1):1–39, 2016. doi: 10.5194/wes-1-1-2016. URL `http://www.wind-energ-sci.net/1/1/2016/`.